LAWRENCE
LIVERMORE
NATIONAL
LABORATORY

LLNL-JRNL-640672

Gamma Shadow Effects on Geomagnetic EMP Rise Time and Amplitude

H. W. Kruger

July 9, 2013

Journal of Radiation Effects, Research and Engineering

Disclaimer

This document was prepared as an account of work sponsored by an agency of the United States government. Neither the United States government nor Lawrence Livermore National Security, LLC, nor any of their employees makes any warranty, expressed or implied, or assumes any legal liability or responsibility for the accuracy, completeness, or usefulness of any information, apparatus, product, or process disclosed, or represents that its use would not infringe privately owned rights. Reference herein to any specific commercial product, process, or service by trade name, trademark, manufacturer, or otherwise does not necessarily constitute or imply its endorsement, recommendation, or favoring by the United States government or Lawrence Livermore National Security, LLC. The views and opinions of authors expressed herein do not necessarily state or reflect those of the United States government or Lawrence Livermore National Security, LLC, and shall not be used for advertising or product endorsement purposes.

Gamma Shadow Effects on Geomagnetic EMP Rise Time and Amplitude

Hans Kruger
Lawrence Livermore National Laboratory

Abstract

The synchrotron radiation based 3D geomagnetic EMP code MACSYNC has been used to explore the effect on EMP rise time and amplitude when a structure is located between the burst point and the observer in an urban setting, producing a gamma shadow. Computations with a 0.1 nanosecond wide gamma output pulse and yields in the 1 – 100 kt range, show that the rise time is stretched to tens of nanoseconds and the amplitude increased by as much as two orders-of-magnitude compared to the amplitude without a gamma shadow. The rise time increase is caused by a reduced creation of radiating Compton electrons near the line-of-sight. The increase in amplitude is due to a reduced ionization density and associated air conductivity in the gamma shadow. These effects potentially impact DOD EMP hardening standards, military applications of EMP, EMP observation from space, and use of EMP for technical forensics.

Introduction

The effects of computing geomagnetic EMP in three dimensions, instead of the one-dimensional treatment used in legacy codes such as CHAP and HEMP, on rise time and shape of the electromagnetic pulse was discussed by the author in a recent JRERE paper for an isotropic gamma source[1]. Currently, the author is exploring the effects due to a three-dimensional gamma source distribution produced when an object located between the source and the observer casts a gamma shadow. This is a progress report on that effort.

Expected effects

In typical nuclear explosion environments, objects located between the warhead and an observer are difficult to avoid. The warhead delivery vehicle itself typically contains various components that will absorb gammas. If the explosion occurs near the ground, structures near the burst point will cast gamma shadows.

The shadowing object will reduce the number of Compton electrons created in the shadow cone and the associated air ionization density and conductivity. This is expected to have two effects. One effect is that EMP travelling to the observer through the shadow cone will experience less attenuation. The other effect is that the reduced

number of radiating Compton electrons near the line-of-sight will reduce the early arriving part of the EMP and thus increase its rise time.

Gamma shadow effects in urban settings

The effects of a gamma shadow on the electromagnetic pulse have been investigated with the author's 3D geomagnetic EMP code MACSYNC for a nuclear ground burst in an urban setting. MACSYNC uses the MCNP code developed by the Los Alamos National Laboratory for coupled gamma-electron Monte Carlo transport.[2] For every electron transport step in MCNP, MACSYNC generates a synchrotron radiation mini-pulse in the direction of the observer. Each mini-pulse is attenuated along the line-of-sight (LOS) to the observer using a preloaded space- and time-dependent air conductivity model. The model includes conduction electron attachment during the interval between ionization creation, at a given radius and angle with the LOS, and traversal of that location by the mini-pulse. At the observer, these attenuated pulses are tallied into time-of-arrival bins and vectorally added to produce the composite electromagnetic pulse. For more details of the MACSYNC synchrotron radiation and conductivity models, see Ref.1.

The urban burst geometry used in MACSYNC is shown in Fig.1. The burst point is at the center of a circular "town square" surrounded by buildings modeled as a circular wall located at 100 meters from the center. The composition of the wall material is SiO_2 with various densities so as to obtain a range of values for gamma transmission through the wall. The baseline computations used a wall height of 36.4 m, chosen to result in a 20 degree angle between the shadow cone and the ground. Some computations were repeated with a 15 or 99 meter high wall. The baseline computations used a gamma energy of 3 Mev and a total yield of 1 kiloton with a 0.3% gamma yield fraction, resulting in ~2.3e+22 gammas per kiloton total yield. A value of 1.2e-3 g/cc was used for the sea level air density.

In the absence of the wall, for a total yield of 1 kt, the air ionization makes the region within a radius of ~1 km opaque to EMP. Any EMP generated within that radius by Compton electrons will be completely absorbed on its way to the observer. The transmission increases for EMP generated at larger radii than 1 km, reaching ~50% at 1.4 km and finally ~100% at 1.9 km (see Fig.2). When the wall is inserted between the observer and the burst, the EMP transmission increases as the gamma transmission through the wall decreases. This is displayed in Fig. 2 for gamma transmission values ranging from 50 to 0.01%.

The reduced conductivity in the gamma shadow, due to a given reduced gamma transmission of the wall, is modeled in MACSYNC by reducing the air conductivity in the shadow cone by the gamma transmission factor whenever the EMP mini-pulse is travelling within the shadow cone on its way to the observer.

The composite EM pulse seen by a distant observer is shown in Fig. 3 for gamma transmission values ranging from 100 to zero percent. The MACSYNC computations used a total yield of 1 kt, a 0.01 shake = 0.1 nanosecond wide gamma output step pulse, and a 0.5 gauss magnetic field perpendicular to the LOS to the observer. The wall height was 36.4 m. It can be seen that the gamma shadow cast by a wall can increase the computed peak field by as much as one order-of-magnitude compared to the field in the absence of the wall.

The 36.4 m wall produced a gamma shadow angle of 20 degrees. The MACSYNC computations for 0.01% gamma transmission, which produced the largest field increase, were repeated for a wall height of 15 m (~8.5 degrees shadow cone angle) and 99 m (~45 degrees). The results for all three wall heights are compared in Fig. 4. A gamma transmission factor of 0.01% requires an areal mass of ~260 grams per square centimeter. This is equivalent to about one meter's worth of concrete or brick construction, which is a reasonable estimate for a city block consisting of two back-to-back apartment buildings.

Finally, the calculations were repeated with 10 and 100 kt total yields for the 0.01% gamma transmission wall. These calculations, along with the corresponding calculation for 1 kt, are shown in Fig.5 and compared with calculations without a wall for the same yields. (In all Figures, the direction of the magnetic field was chosen to make the main pulse positive. Also, in all Figures, except the upper Figure 5, a very small negative tail, lasting a few hundred shakes, was suppressed in order to enable logarithmic plots.)

It is well known, that in the absence of a gamma shadow, the air conductivity severely limits field increases as the yield is increased. As the yield changes from 1 to 10 or 100 kt, the EMP-opaque radius changes from ~1 km to ~1.3 or ~1.6 km. As a result, the volume from which EMP can escape to the observer is reduced, however, at the same time the density of radiating Compton electrons is increased proportional to the yield. These two effects almost cancel, causing the peak field to saturate. However, in the presence of a wall with little gamma transmission, there is little air conductivity to offset the increase in Compton electron density, and the field continues to rise significantly as the yield increases, as can be seen in Fig. 5. The field in the shadow cone is larger by a factor of ~40 for 10 kt and ~100 for 100 kt than the field without the gamma shadow, for the same yields.

In these calculations, MACSYNC was set up with MCNP tally zones consisting of 100 m wide spherical shells from 100m to 2 km. This made it possible to identify the contributions to the composite field at the observer from the different zones. Fig. 6 shows these contributions for the 100 kt calculations displayed in Fig.5. It can be seen from Fig. 6, that zones from ~1.6 km inward do not contribute to the initial field in the absence of a gamma shadow, and this changes only later in the pulse when attachment has reduced the conduction electron density (the attachment time constant is ~ 1 shake). Zones inside ~1 km never contribute to the EMP at all. By contrast, when the gamma transmission is only 0.01%, all cells contribute from the beginning of the pulse. However, the onset of that pulse is delayed because radiating electrons near the LOS are missing and the sources are located instead near the gamma cone surface. The

reason for this delay is that, for these sources, the combined path length of the gammas to the Compton scattering site and of the EM radiation from that site to the observer is longer than for Compton electrons generated near the LOS.

All of the sources contributing to the increases in EMP amplitude, for a shadow cone scenario with very low gamma transmission, are created at distances so close to the burst that radiation emitted by them would be significantly attenuated in the absence of the shadow. One of these sources consists of Compton electrons produced by previously unscattered gammas outside of the cone, but close enough to its surface so that its radiation can escape complete EM attenuation before reaching the surface. This radiation will then experience greatly reduced additional attenuation inside the shadow cone on its way to the observer. A second source will be Compton electrons radiating inside the shadow cone after crossing into it from the unshadowed region. A third source consists of Compton electrons created inside the shadow cone by scattered gammas crossing over into the cone. This source will contribute to the composite EMP only at late times. The spherical shell tally zones used in these computations cannot provide any information about the relative contribution of these three sources to the total composite EMP.

Discussion of Results

Both the delay and increase in EMP rise time due to a gamma shadow computed by MACSYNC are consistent with expectations based on simple first-principles considerations.

MACSYNC computations of the peak field with a gamma shadow show an increase by as much as an order-of-magnitude for a 1 kt and two orders-of-magnitude for a 100 kt yield, compared to the field in the absence of a gamma shadow. An increase in the peak field is expected from first principles, given the reduced conductivity in the shadow cone, however, there appears to be no means for a simple first-principles estimate of the expected magnitude of such an increase. Thus the question needs to be asked whether the physics simplifications used in MACSYNC could be responsible for much of the observed field increase.

The physics simplifications are:

1. Non-self-consistency -
   Since the field at the observer is not known until all the gammas and their Compton electrons have been transported, one at a time, the electromagnetic field is unknown during the MACSYNC computations. Furthermore, only the radiated far field, not the close-in conduction field, is computed. Both of these conditions prevent treatment of the effect of the self-fields on the motion of the Compton electron and on the field-dependent conduction electron mobility and attachment rate.

2. Neglect of air breakdown –
   Avalanching of conduction electrons, potentially leading to air breakdown, also cannot be treated because the fields are unknown.

3. Discontinuous air mobility at the shadow cone boundary –
   For each EM mini-pulse propagation step between the radiating Compton electron and the observer, the conductivity used for attenuation computation is a fixed fraction, equal to the wall's gamma attenuation factor, of the unshadowed conductivity, while the mini-pulse is propagating within the shadow cone. Thus the conductivity is treated as discontinuous at the cone surface. In reality, the conductivity is feathered across the cone surface because of Compton electron transport across the surface at early times and scattered gammas crossing the surface at late times.

The static breakdown threshold for sea level air is ~3 Megavolts per meter.[3] In order for avalanching to short out the EMP prior to the observed peaks, say a few nanoseconds into the pulse, the field needs to be ~5 MV/m, based on high-power microwave propagation computations and measurements.[4] The conduction electron avalanche leading to air breakdown is initiated by electrons naturally occurring in the atmosphere due to cosmic rays and background radioactivity. Close to the burst, the density of these seed electrons will be increased over their background value by gammas and neutrons from the nuclear weapon. However, the air breakdown threshold is relatively insensitive to seed electron density based on experiments conducted in the gamma and neutron flux of a nuclear reactor. The measured breakdown threshold was ~20% lower in the reactor radiation environment than in the ambient sea level air.[5] The largest distance-field product seen in the current computations is ~5e+9 Volt for a 100 kt yield, producing ~2.5 MV/m just outside the bulk of the source region at a distance of 2 km. This is below the breakdown threshold. Thus air breakdown is unlikely to appreciably reduce the peak fields computed for the yields and scenario used in this paper. (However, had this EMP been generated in a high-altitude burst, air breakdown would have clamped the field at a much lower value since the breakdown threshold is proportional to air density.)

The discontinuous air conductivity model is also unlikely to be responsible for the large fields observed in the gamma shadow because the quantity determining EM attenuation is not the detail of the variation of the conduction electron density with distance, but rather the line integral of the electron density. However, the integral of the conduction electron density along the instantaneous LOS between the radiating Compton electron and the observer is, at least to first order, the same whether the energy deposition is uniform up to the cone surface, as assumed in the MACSYNC treatment, or smeared out across it.

Non-self-consistent treatment of the Compton electron motion is also not likely to have caused the large observed fields, because Conrad Longmire has shown that the effects of self-electric and self-magnetic fields cancel another, to first order.[6]

Finally, there is the issue of neglecting the self-electric field on conduction electron mobility and attachment rate. MACSYNC uses a constant value of 0.3 meter/sec per Volt/meter for the mobility and a constant attachment time of 1 shake = 10 nanoseconds. These are reasonable approximations for the range of self-fields computed in the absence of a gamma shadow. For the larger self-fields seen in the gamma shadow, the mobility decreases and the attachment time increases.[7] Between the opposing effects of these two changes on conductivity, the mobility decrease should dominate since the conductivity will respond instantaneously to a decreased mobility, however, previously attached conduction electrons will not become detached when the field increases. Thus use of the mobility and attachment rate values for the lower fields will somewhat overestimate the conductivity and associated EM attenuation and for this reason cannot be responsible for the computed large field increases.

In summary, none of the physics simplifications used in MACSYNC appear to be capable of producing the large EM field increases computed by the code when a shielding material casts a gamma shadow.

Conclusions and Observations

MACSYNC calculations presented in this paper show that the gamma shadow cast by a typical city block, consisting of two parallel rows of brick apartment buildings, will stretch the rise time of the EMP, produced by delta function gamma output pulses from nuclear bursts with yields in the range from 1 – 100 kt, to tens of nanoseconds and increase its amplitude by as much as two orders-of-magnitude compared to the amplitude in the absence of a gamma shadow. This amplitude increase is caused by the reduced ionization density and associated conductivity in the gamma shadow which forms an electromagnetic leakage channel. The rise time increase is caused by a reduced creation of radiating Compton electrons near the LOS.

This EMP rise time increase will make it difficult to deduce the rise time of a fast gamma pulse from its EMP signal in an urban environment that blocks a direct view of the burst. It will also make it more difficult to detect, within a gamma shadow, the EMP generated by such a burst from space platforms, since efficient penetration of the ionosphere requires a fast rise time.

The computed EMP amplitudes exceed the amplitude specified in current DoD EMP hardening standards by as much as two orders-of-magnitude.[8]

Similar effects on EMP rise time and amplitude are likely to occur in other surface or high-altitude burst scenarios involving gamma shadows. Since the impact of such effects on hardening standards and various National applications of EMP is potentially significant, it appears advisable to verify the predictions of the MACSYNC code, which uses synchrotron radiation superposition to arrive at the composite geomagnetic EMP,

with a code using the more traditional method of computing the currents and solving Maxwell's equations on a spatial grid. This requires a 3D code with detailed coupled gamma-electron transport, very high spatial resolution, self-consistency, and air avalanche treatment. Such a code, which does not exist today, ought to be developed. It also appears advisable to explore the feasibility of experiments that could validate the computed gamma shadow effects on EMP.

Acknowledgement

The author thanks Dr. David Larson for his encouragement and support, and Robert Palasek for assistance with programming and compilation issues.

Prepared by LLNL under Contract DE-AC52-07NA27344

References

1. H. Kruger, "3D Effects in Geomagnetic EMP Computations", Journal of Radiation Effects, Research and Engineering, Vol. 31, No. 1, 159 (2013).
2. Los Alamos National Laboratory X-5 Monte Carlo Team, "MCNP – A General Monte Carlo N-Particle Transport Code, Version 5", LA-UR-03-1987, 2005.
3. H. P. Westman, editor, "Reference Data for Radio Engineers", Fourth Edition, American Book – Strafford Press Inc., p. 921 (1960).
4. D. L. Fenstermacher and F. von Hippel, "An Atmospheric Limit on Nuclear-powered Microwave Weapons", Science & Global Security, Vol. 2, p. 310 (1991).
5. G. I. Duncan et al, "The Effects of Nuclear Radiation on the Electrical Strength of Air", Trans. Amer. Inst. Elect. Engrs., Part I, Vol. 79, p. 19 (1960).
6. C. L. Longmire, "The Early-Time EMP from High-Altitude Nuclear Explosions", Mission Research Corporation Report MRC-R-809, p. 66, 1983.
7. M. K. Grover and F. R. Gilmore, "A Review of Data for Electron Mobility, Energy, and Attachment Relevant to EMP Air Chemistry", R&D Associates report RDA-TR-110002-0001, March 1979.
8. Department of Defense Interface Standard, Electromagnetic Environmental Effects Requirements for Systems MIL-STD-464, 18 March 1997.

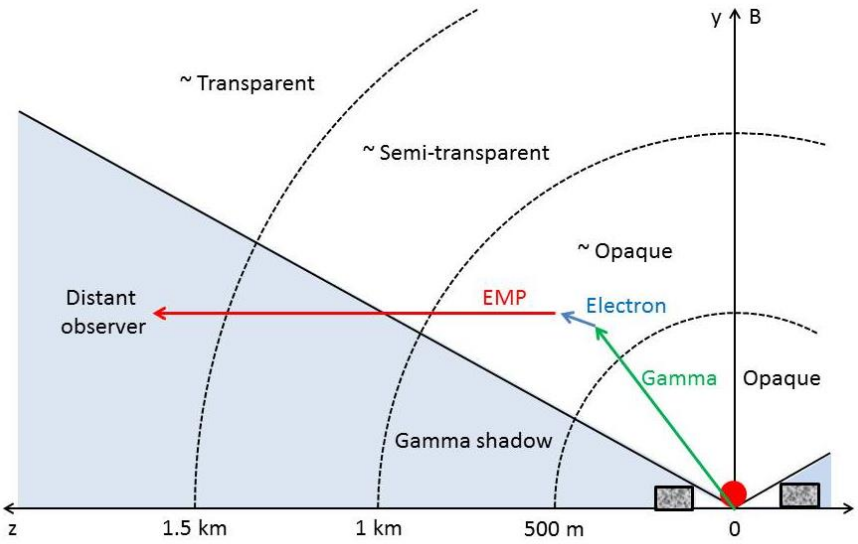

Fig. 1. Geometry used in MACSYNC for a nuclear burst in an urban scenario. The distant observer is located on the z-axis. The burst is at the center of a circular “town square” surrounded at 100 m by buildings represented by a circular wall with heights of either 15, 36.4, or 99 m, 100m wide, made of SiO_2 of various densities corresponding to a range of gamma transmission.

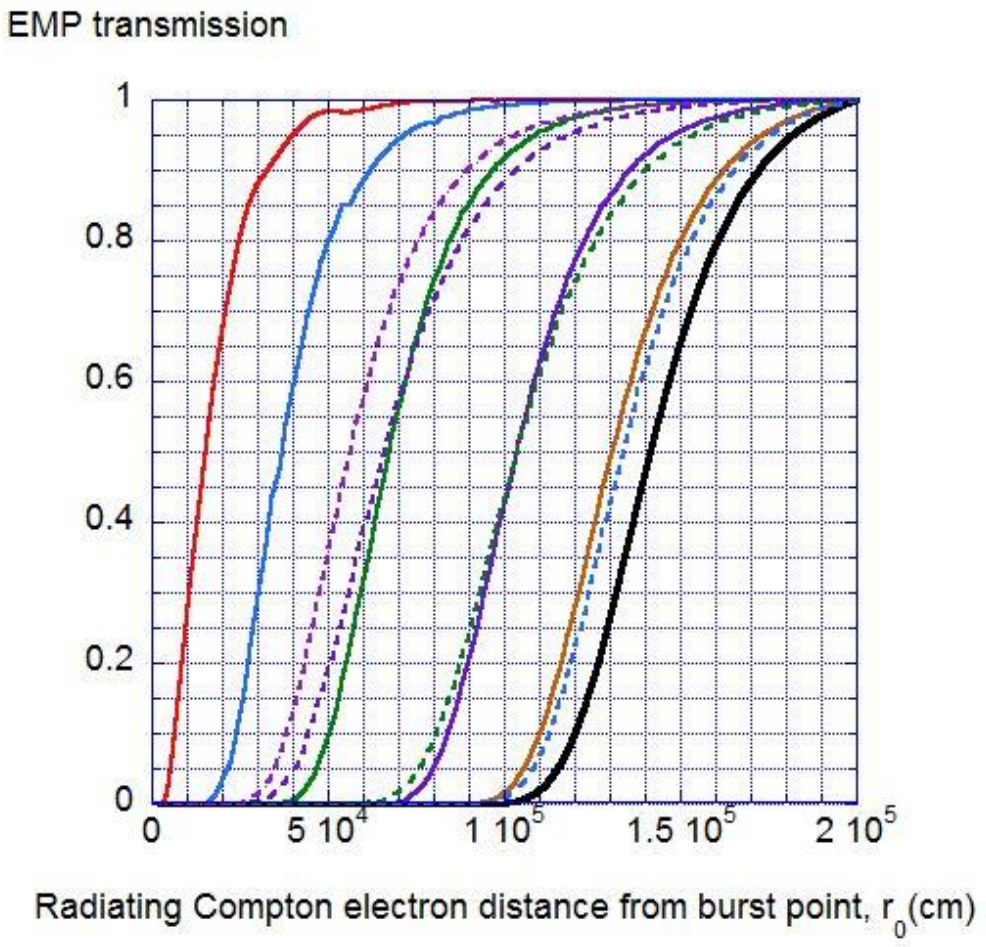

Fig. 2. EMP transmission from a radiating Compton electron located on the z-axis at r_0 from the burst. The different solid curves, from right to left, correspond to wall gamma transmission of 100, 50, 10, 1, 0.1, and 0.01%. The total yield is 1 kt with a 0.3% yield of 3 Mev gammas emitted in a step output pulse 0.01 shakes wide, where 1 shake equals 10 nanoseconds. The dashed curves, from right to left, correspond to 100% gamma transmission and times after the gamma pulse of 1, 10, 100, and 1000 sh, when conduction electron attachment has reduced the air conductivity. The attachment time constant is 1 sh.

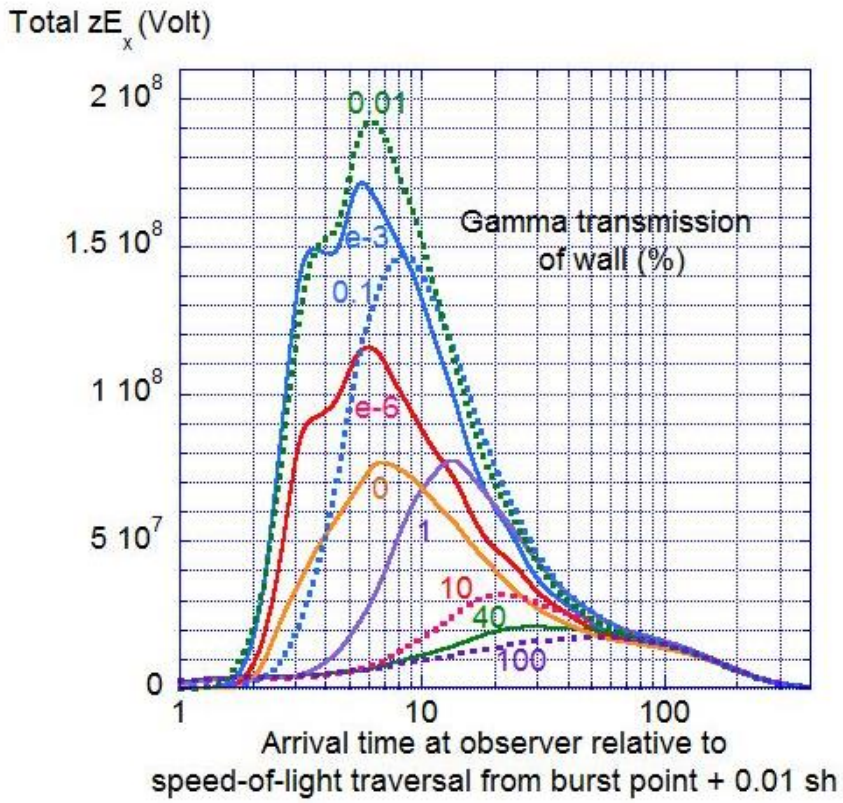

Fig.3. EMP for a wall height of 36.4 m. The total yield is 1 kt with an 0.3% yield of 3 Mev gammas emitted in a step output pulse 0.01 shakes wide. There is a 0.5 gauss magnetic field perpendicular to the line-of-sight. (Time in units of shakes.)

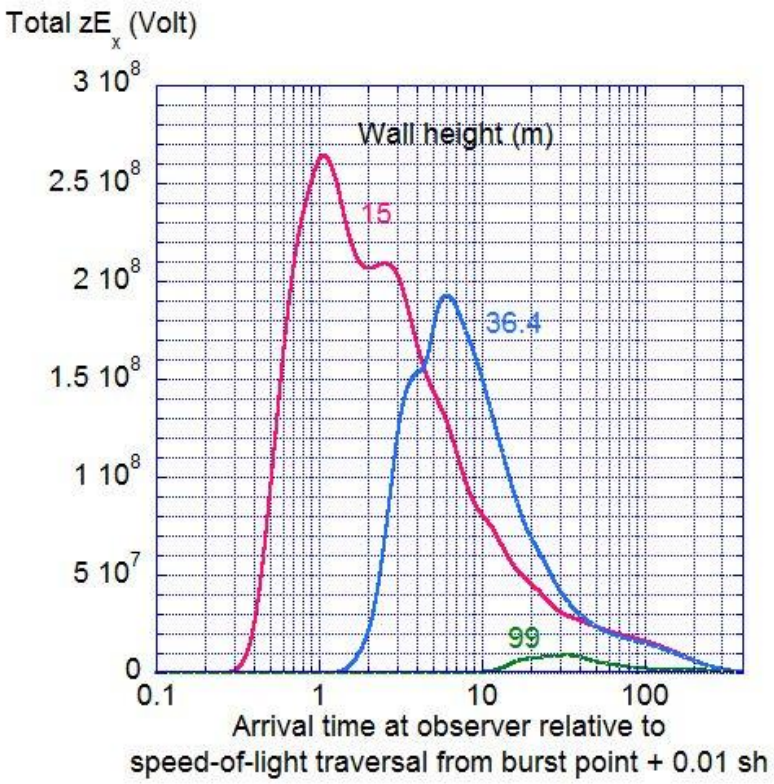

Fig. 4. EMP for wall heights of 15, 38.4, and 99 m. The gamma transmission is 0.01%. Other parameters are the same as in Fig. 3. (Time in units of shakes.)

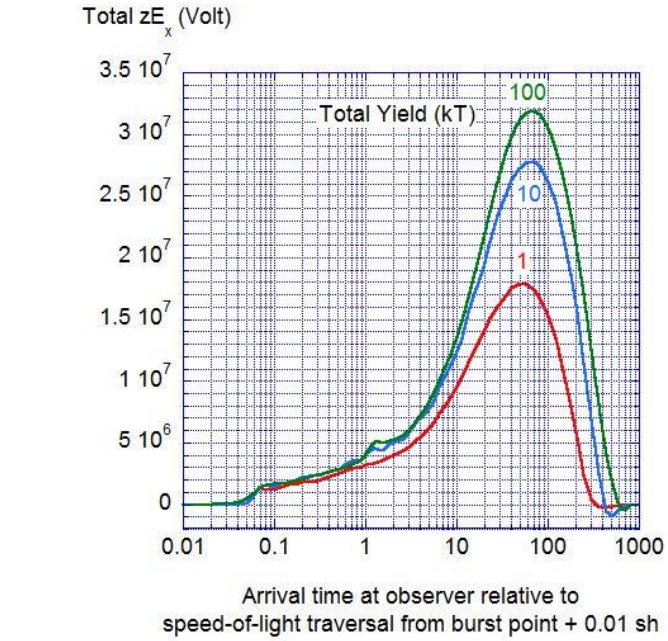

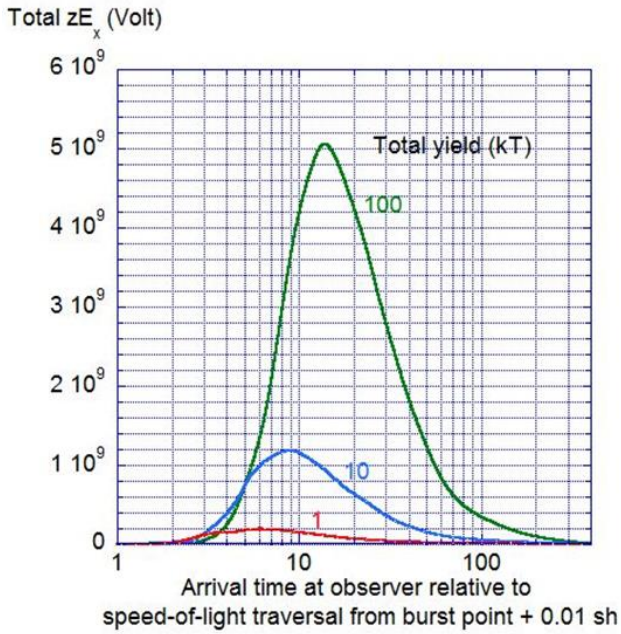

Fig. 5. The upper plot is for a wall gamma transmission of 100% and the lower plot for 0.01% transmission. The wall height is 36.4 m. Other parameters are the same as in Fig. 3. (Time in units of shakes.)

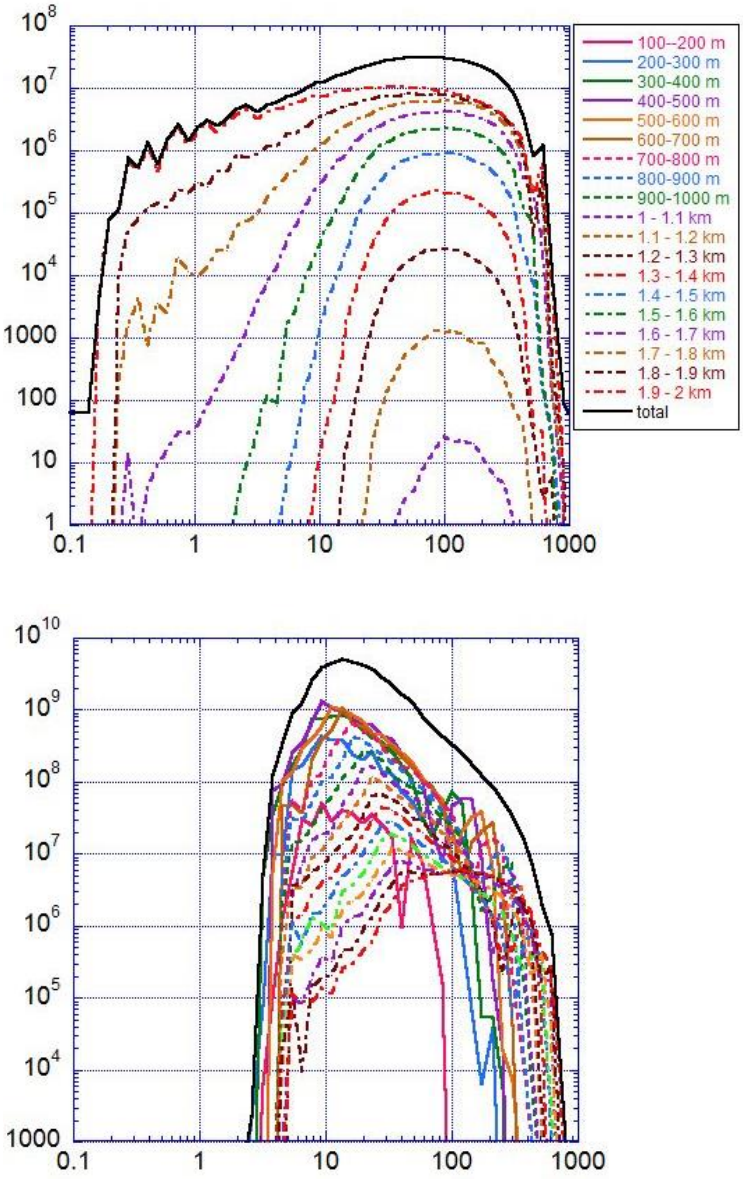

Fig. 6. Contributions to total EMP from 100 m wide spherical shells of air, starting at a radius of 100 m, for the 100 kt plots shown in Fig. 5. The upper plot is for a wall gamma transmission of 100% and the lower plot for 0.01% transmission. The wall height is 36.4 m. Other parameters are the same as in Fig. 3. The vertical axis is the distance-field product in units of Volts. The horizontal axis is the arrival time at the observer relative to speed-of-light traversal from the burst point with a 0.01 shake offset (in units of shakes).